Evaluation and Bias-Correction of Dynamically Downscaled Climate Projections

Guillaume Mauger, Jason Won

University of Washington Climate Impacts Group

Mar 2024

TABLE OF CONTENTS

CITATION: Mauger, G.S. and J.S. Won 2024. Evaluation and Bias-Correction of Dynamically Downscaled Climate Projections. Report prepared for the Puget Sound Partnership. Climate Impacts Group, University of Washington.

FUNDING ACKNOWLEDGEMENT: This project has been funded wholly or in part by the United States Environmental Protection Agency under assistance agreement PC-01J95801-2 to the Washington State Department of Ecology. The contents of this document do not necessarily reflect the views and policies of the Environmental Protection Agency, nor does mention of trade names or commercial products constitute endorsement or

Purpose

The current version of the Stormwater Heatmap includes one dynamically downscaled projection, based on the GFDL-CM3 model. There are two limitations to the current approach. First, it is based on just one climate model projection. Given that there is no way to objectively rank one climate change projection over another, best practices in climate change analysis suggest analyzing the potential effects of multiple projections (e.g., Ransom et al., 2018). Second, the results for the GFDL-CM3 model projection were used directly, without any correction for biases. Recent work has identified biases in these projections that must be corrected prior to use in hydrologic modeling (e.g. Mauger et al. 2021). The purpose of this project was to improve on the climate projections in the Stormwater Heatmap tool by addressing these two limitations. Specifically, we developed an ensemble of dynamically downscaled projections, bias-corrected based on comparisons with observations.

Background

Stormwater Heatmap

This Stormwater Heatmap was developed by The Nature Conservancy, Geosyntec Consultants, and Cheva Consultants with collaboration from the UW Climate Impacts Group, the Washington Department of Fish & Wildlife, and the NOAA Office of Coastal Management. Funding was provided by The Boeing Company.

The tool estimates runoff and associated water quality issues across the lowlands of Puget Sound. Runoff estimates are developed using the Hydrologic Simulation Program FORTRAN (HSPF). Model parameters for the Puget Lowlands were originally calibrated by Dinicola et al. (1990), then updated by Clear Creek Solutions (Department of Ecology, 2014). In addition to modeling estimates of runoff, the team uses linear mixed-effects models to estimate pollutant loadings for a range of water quality metrics. All results are pre-calculated for distinct hydrologic response units and are aggregated using a lookup table approach, which facilitates rapid visualization and allows others to estimate local runoff and water quality conditions under different land cover or management scenarios.

Dynamically Downscaled Projections

“Downscaling” refers to methods that relate coarse scale global climate model (GCM) projections to local-scale changes of relevance to management. Past research has primarily used “statistical downscaling”, which relies on empirical relationships between weather observations and GCM output. Recent research has shown that “dynamical downscaling”, in which a regional climate model is used to downscale GCM projections, can more accurately represent changes, particularly for extreme precipitation and in areas with complex topography (Salathé et al. 2014). This work leverages existing dynamically downscaled datasets that have been developed in recent years (Chen et al. 2018, Mass et al. 2022). These are described in more detail below.

Observed Data

Reference Datasets

We considered four sources of observational data for evaluating the model projections (Table 1). Initial evaluation revealed that the Quantitative Precipitation Estimates (QPE) and Integrated Multi-satellitE Retrievals for GPM (IMERG) datasets were not suitable for use in this study. The IMERG results showed very little spatial detail as well as non-sensical results for most of the metrics considered. For instance, the climatology for Oct-Dec precipitation from IMERG showed none of the spatial detail present in the other two datasets, in spite of well-documented and significant gradients across the Puget Sound catchment. The QPE data appeared reliable but the available record for Puget Sound was too short to provide statistically robust comparisons. Although the national dataset spans from 2002-2023, most is missing data for Puget Sound, leaving only a little over 2 years of valid data (Apr-Jun 2003, Jun 2019 - Jun 2021). We deemed this insufficient for evaluating the dynamically downscaled projections. As a result of eliminating these two datasets, all gridded comparisons were made using the daily gridded meteorology from the Parameter Regression on Independent Slopes Model dataset (PRISM, Daly et al. 2008, Daly et al. 2021).

Table 1. Reference datasets to be evaluated for use in bias correcting the dynamically downscaled projections.

Name	Resolution	Years	Citation
Parameter Regression on Independent Slopes Model (PRISM)	800 m / Monthly	1991-2020	Daly et al. 2008
National Centers for Environmental Prediction (NCEP) National Stage IV Quantitative Precipitation Estimate (QPE) Product	4 km / Hourly	2002-2023	Nelson et al. 2016
National Aeronautics and Space Administration (NASA) Integrated Multi-satellitE Retrievals for GPM (IMERG)	0.1° / 30 min	2000-2021	Huffman et al. 2018
Weather station data (ds3505; see Table 2)	N/A / Hourly	varies	N/A

We also used hourly precipitation measurements from weather stations to perform point comparisons with the dynamically downscaled projections (Table 2, Figure 1). These were obtained from the “Global Hourly” dataset (ds3505) in the NOAA Integrated Surface Database (ISD). All of the stations identified are part of the Automated Surface Observing Systems (ASOS) network, which was designed to monitor weather conditions at airports. We extracted field “AA1”, corresponding to “LIQUID-PRECIPITATION” from the data files. All data provided by NOAA include data quality flags that can be used to process the data. We filtered out any data with a "condition code" other than Trace. For "Trace", we assumed zero precipitation. For the "quality code", we removed all data except those flagged as "Passed all quality control checks".

Table 1. Weather stations used in the analysis. All sites include hourly precipitation data and were obtained from the "Global Hourly" dataset (ds3505) in the NOAA Integrated Surface Database (ISD).

Station	ID	Latitude	Longitude	Years
Bellingham	72797624217	48.794N	122.537W	1973-present
Bremerton	72792894263	47.483N	122.767W	2006-present
Friday Harbor	72798594276	48.522N	123.023W	2006-present
Olympia Airport	72792024227	46.973N	122.903W	1973-present
Quillayute	72797094240	47.938N	124.555W	1973-present
Quinault	99999904237	47.514N	123.812W	2006-present
SeaTac	72793024233	47.445N	122.314W	1948-present

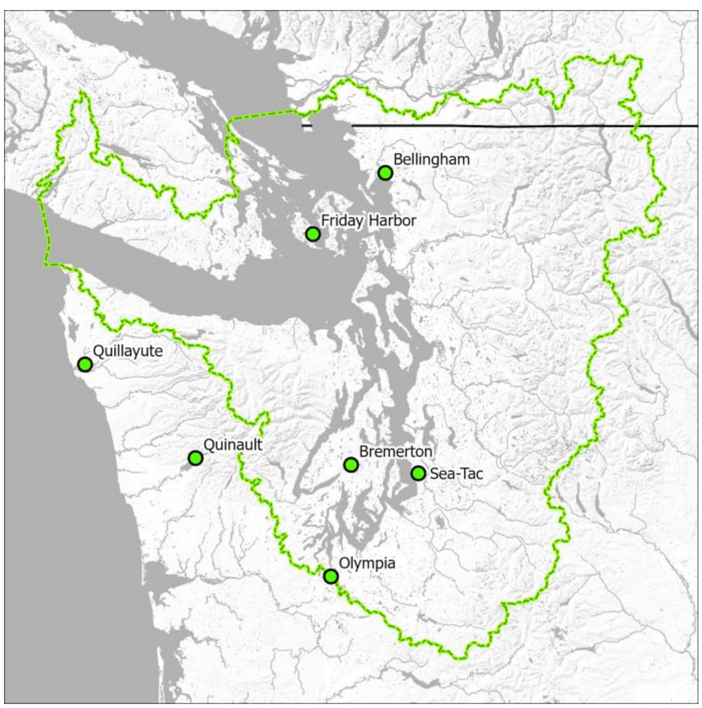

Figure 1. Map showing the locations for the weather stations used in the analysis. The Puget Sound domain is outlined in green.

Model Data

Global Climate Model (GCM) Projections

GCM projections were obtained from the Climate Model Inter-comparison Project, phase 5 (CMIP5; Taylor et al., 2012). The twelve GCMs included in the WRF ensemble (Table 1) were chosen based on Brewer et al. (2016), who selected GCMs by prioritizing which model would be selected from each modeling center, as follows: (i) selecting the higher resolution model for each modeling center, and (ii) selecting models with the best agreement with observations of surface temperature, sea level pressure, and 500 hPa geopotential heights in the Pacific Northwest region. We note that other approaches to ranking could come up with different rankings (e.g. Rupp et al. 2013), though research suggests that it is most important to include an ensemble of models (e.g. Brekke et al. 2008). Brewer et al. (2016) identified 17 GCMs in total, but only 12 included the variables needed to provide boundary conditions to the regional climate model, described below.

Additional information on model evaluation and ranking is summarized in Mauger and Won (2019). In addition, Mauger and Won (2019) discuss approaches for using RCP 8.5 projections as an analog for what might be projected for the RCP 4.5 scenario. For example, the 2080s in the RCP 4.5 projections appear to correspond approximately to the 2040s or 2050s in the RCP 8.5 projections.

Regional Climate Model

Regional Climate Model simulations were produced using the Weather Research and Forecasting (WRF, http://www.wrf-model.org; Skamarock et al., 2005) community mesoscale model. We used two WRF datasets:

1. An observationally based historical simulation developed by PNNL (Chen et al. 2018), driven by meteorological fields obtained from the North American Regional Reanalysis (NARR; https://www.esrl.noaa.gov/psd/data/gridded/data.narr.html). This simulation was developed using WRF version 3.8 and implemented at a spatial resolution of 6 km spanning the years 1981-2020. Hereafter referred to as “WRF-NARR”.
2. An ensemble of 12 WRF projections (Mass et al. 2022), driven by global climate projections obtained from the Coupled Model Intercomparison Project Phase 5 dataset (CMIP5; Taylor et al. 2012; http://cmip-pcmdi.llnl.gov/cmip5/). These simulations were implemented using WRF version 3.8 at a spatial resolution of 12 km, spanning the years 1970-2099. Hereafter referred to as “WRF-CMIP5”.

Table 2. The twelve global climate models (GCMs) used as input to the regional model simulations. All simulations are based on the high-end RCP 8.5 greenhouse gas scenario (Van Vuuren et al., 2011).

Model	Center	Resolution (degrees)	Vertical Levels
ACCESS1-0	Commonwealth Scientific and Industrial Research Organization (CSIRO), Australia/ Bureau of Meteorology, Australia	1.25 x 1.88	38
ACCESS1-3	Commonwealth Scientific and Industrial Research Organization (CSIRO), Australia/ Bureau of Meteorology, Australia	1.25 x 1.88	38
bcc-csm1-1	Beijing Climate Center (BCC), China Meteorological Administration	2.8 × 2.8	26
CanESM2	Canadian Centre for Climate Modeling and Analysis	2.8 × 2.8	35
CCSM4	National Center of Atmospheric Research (NCAR), USA	1.25 × 0.94	26
CSIRO-Mk3-6-0	Commonwealth Scientific and Industrial Research Organization (CSIRO) / Queensland Climate Change Centre of Excellence, Australia	1.8 × 1.8	18
FGOALS-g2	LASG, Institute of Atmospheric Physics, Chinese Academy of Sciences	2.8 × 2.8	26
GFDL-CM3	NOAA Geophysical Fluid Dynamics Laboratory, USA	2.5 × 2.0	48
GISS-E2-H	NASA Goddard Institute for Space Studies, USA	2.5 × 2.0	40
MIROC5	Atmosphere and Ocean Research Institute (The University of Tokyo), National Institute for Environmental Studies, and Japan Agency for Marine-Earth Science and Technology	1.4 × 1.4	40
MRI-CGCM3	Meteorological Research Institute, Japan	1.1 × 1.1	48
NorESM1-M	Norwegian Climate Center, Norway	2.5 × 1.9	26

In both cases, the driving data (NARR, CMIP5 GCMs) provides the initial and boundary conditions for the WRF model simulations.

The new ensemble of WRF projections includes one simulation for each of the GCMs listed in Table 2, all based on the high-end RCP 8.5 greenhouse gas scenario (Van Vuuren et al., 2011). All simulations are archived at an hourly time step. Model outputs include a spatially gridded time-series of meteorological variables: temperature (°C), relative humidity (%), precipitation (mm), wind speed (m/s), and incoming short- and long-wave radiation (W/m2), among others.

Approach

Evaluation

All comparisons with observations focused on the WRF-NARR simulation, since it is forced by observed conditions (in contrast, the CMIP5 simulations are "free running" and do not match the time series of observed weather and climate conditions). We compared gridded estimates of both seasonal and extreme precipitation. Seasonal totals were compared for Oct-Dec, Jan-Mar, Apr-Jun, and Jul-Sep. These groupings were selected because they generally align with the climatology of precipitation, in particular the dry season, which is centered around August for Puget Sound. We compared the following quantiles of daily precipitation: 75^{th}, 90^{th}, 95^{th}, 99^{th}, 99.5^{th}, and 99.9^{th}. These were calculated using a standard empirical quantile estimator ((r-0.5)/n). For the point comparisons we explored the same seasonal totals and quantiles, and also compared the full probability distribution, total accumulation for discrete intensity bins, the lag correlation in hourly precipitation, and correlations for different precipitation durations.

Bias Correction

Bias-correction techniques can introduce spurious trends in climate projections, resulting in erroneous impacts projections for the future. To avoid such errors, we only apply corrections that are time-invariant in their effects. Since we anticipate that biases will not be the same for all precipitation intensities, we use the "percentile-delta" bias correction approach, developed by Mauger et al. (2016). In this approach, different corrections are applied to different precipitation intensities, binned so as to ensure an adequate sample size. In our case, we used PRISM daily precipitation to bias-correct WRF daily precipitation totals, applying the same scaling to all hourly precipitation totals within each day. PRISM daily precipitation is based on the 24 hour total between 12pm and 12pm Universal Time for each day. We did not align this with the WRF definition of daily precipitation, which is based on local standard time (midnight to midnight), meaning that there is a four hour offset between these two definitions. Future work should align these to ensure the timing is consistent.

The bias correction approach can be applied seasonally (e.g. with a moving window approach) if biases are found to vary by time of year. We found no evidence of a seasonal dependence in biases, which makes sense given that the mechanisms governing precipitation in the Puget Sound region are fairly consistent year-round. As a result, we did not apply a seasonally based correction.

We do not remove any trends prior to bias correction, in part because precipitation trends are not linear. This means that future precipitation events, which may exceed the maximum historical observation, are bias-corrected according based on the scaling obtained for the 99th-100th percentile. This could be a limitation in our current approach, since biases are likely more closely tied to the dynamics of storm events (e.g. pressure, winds) as opposed to their thermodynamic properties (e.g. precipitation intensity). The dynamics of storms are not projected to change appreciably, whereas precipitation intensity is projected to increase. Additional analysis would be needed to understand the implications of this assumption.

The WRF results often exhibit precipitation that is below the "Trace" threshold typically used in observational records. To correct for this, we applied an additional correction, after bias correction, in which we zero out any hourly precipitation totals that are below a 0.1 mm/hr. This threshold was determined in previous work based on the percentile at which hourly weather station observations transition from zero to non-zero precipitation.

Finally, the WRF-CMIP5 simulations are bias-corrected but not evaluated in this study. Instead, we test the effectiveness of the bias-correction method using WRF-NARR, then apply the same approach to the WRF-CMIP5 results. New scalings are derived for each individual WRF-CMIP5 GCM projection, based on comparisons for the years 1981-2020. These distinct scalings are then applied to the full record (1970-2099) for each WRF-CMIP5 projection. As noted above, no trends were removed prior to bias correction.

Results

Gridded comparisons

Maps comparing total precipitation for each season are shown in Figure 2 for the uncorrected WRF-NARR results. These show that WRF-NARR generally reproduces the magnitude and spatial distribution of seasonal precipitation across the region. Some biases

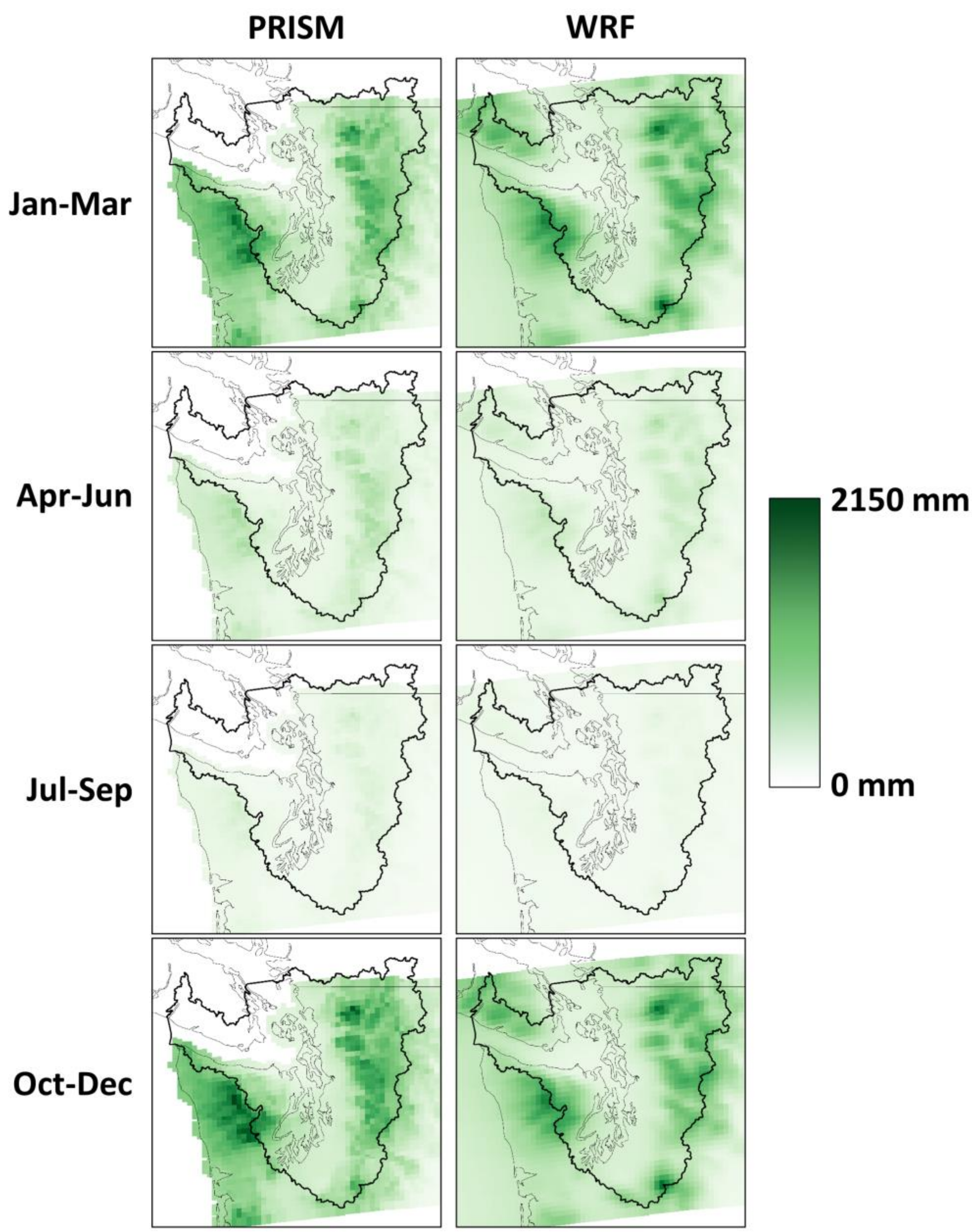

Figure 2. Maps comparing seasonal total precipitation for PRISM (left) and WRF-NARR (right). The Puget Sound domain is outlined in black.

are nonetheless evident, with WRF-NARR precipitation generally appearing to underestimate precipitation across most of the domain, except in the lee of the Olympics where WRF-NARR estimates are biased high. Results for the extremes in daily precipitation (Figure 3) are generally consistent with the seasonal biases, although there are some areas – including parts of the North Cascades, the Willapa Hills, and Mt Rainier – where WRF-NARR appears to overestimate the amplification of precipitation over to the topography.

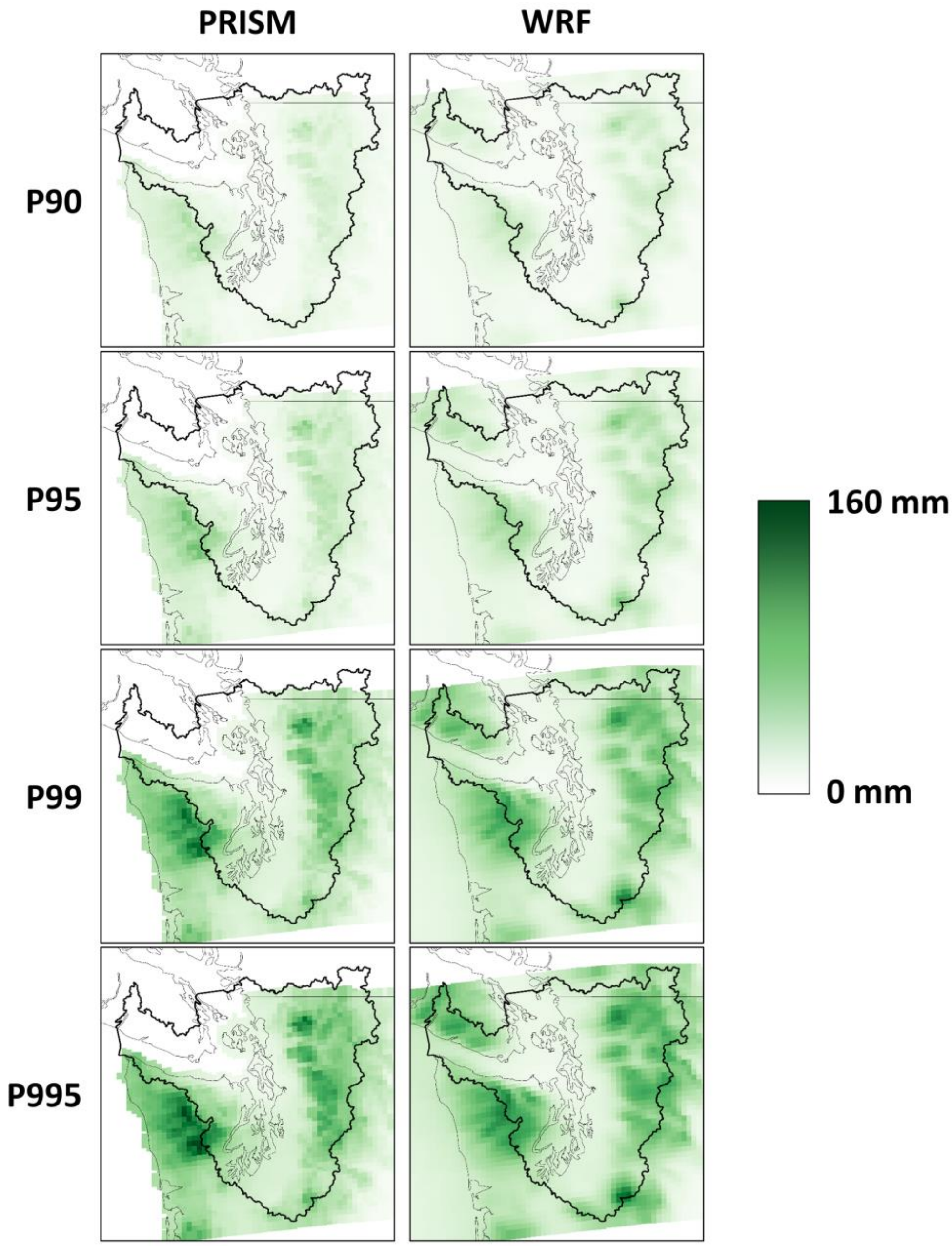

Figure 3. As in Figure 2 except showing the 90th, 95th, 99th, and 99.5th percentiles in daily precipitation.

The WRF-NARR overestimates in the lee of the Olympics are even more pronounced than in the seasonal comparisons. These biases appear to be generally consistent with those found in other WRF datasets (e.g. Rasmussen et al. 2023, Liu et al. 2017). Finally, it is worth emphasizing that PRISM is an interpolated dataset and may also have biases. This means that disagreements between WRF and PRISM could be a result of biases in either dataset.

Point comparisons

Figure 4 shows the correlations between observed and WRF-NARR precipitation for Sea-Tac. These show that hourly precipitation from WRF-NARR is poorly correlated with observations, but that there is no major lag in its precipitation estimates. We initially hypothesized a lag due to the construction of the regional climate model simulations – since observed conditions are imposed at the model boundary, it is expected that the timing and location of events will vary slightly relative to the observations. Although timing differences are undoubtedly present, our lag correlations show that they are not systematically biased one way or another. We also compared correlations for different durations. As the plot shows, correlations increased systematically with duration, with the largest improvements going from 1-hour to 24-hour accumulations. This suggests that time series comparisons with the WRF-NARR data are best applied to daily or longer durations.

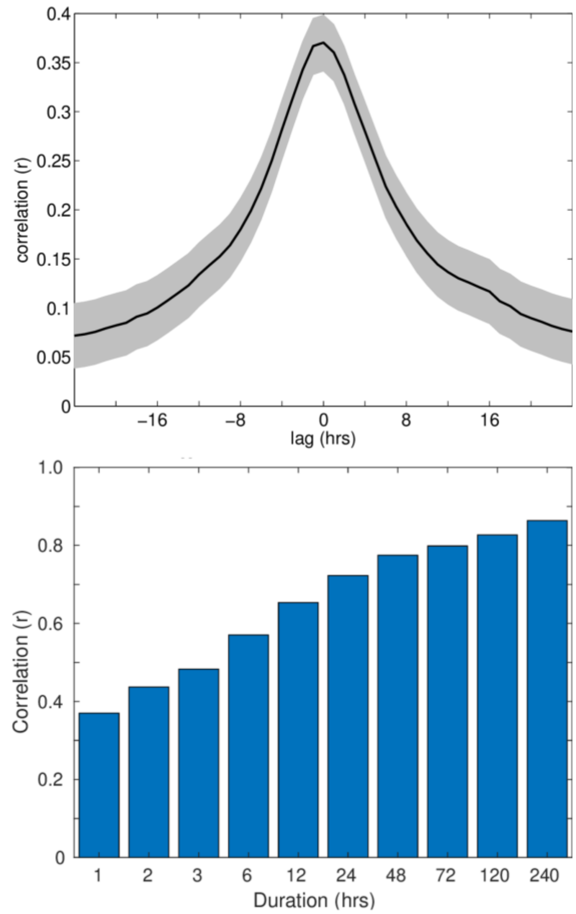

Figure 4. Correlation between observed precipitation at Sea-Tac and the WRF-NARR estimates for the closest grid cell.

Timing is not the only measure of accuracy. For stormwater applications, a more important metric is the probability distribution of precipitation intensities. One way to evaluate this is to compare observed and modeled precipitation in a so-called “Q-Q” plot, in which the ranked data for each are compared. This is the same as comparing the probability distributions but provides an easier way of viewing the differences between the two. Another way to consider distributional biases is to evaluate the total precipitation that falls at different intensities. To do this we calculated the fraction of precipitation that falls in specific intensity bins, ranging up to the maximum observed hourly intensities. Both comparisons are shown below for Sea-Tac (Figure 5). These show that hourly precipitation from WRF-NARR is biased low across most intensities for the Sea-Tac location. This is confirmed in the binned precipitation comparison, which further shows that WRF-NARR has too much low-intensity precipitation and too little high-intensity precipitation. Although not shown, we found that these biases are consistent across all seasons, with no notable differences for different times of year.

It is important to note that these comparisons are imperfect because they compare point observations to grid-averaged model estimates by PRISM and WRF-NARR. Due to the spatial averaging in the model estimates, we expect the extremes to be less pronounced than in the point observations from surface weather stations. This is especially true for the WRF-NARR simulations (6 km resolution), but is likely true as well for the PRISM results (800 m resolution). Future work could use an “areal reduction factor” to address this issue (Kao et al. 2020).

As noted above, we evaluated biases for six other stations in addition to Sea-Tac. Figure 6 compares select quantiles for six ASOS weather stations against PRISM and WRF-NARR estimates for the same locations (in this and all subsequent plots, results for the Quinault station were omitted because the results were similar to those for Quillayute). Consistent with the bias maps shown above, we found that (1) WRF-NARR is generally biased low, (2) biases are different across precipitation intensities, and (3) the biases are not the same for

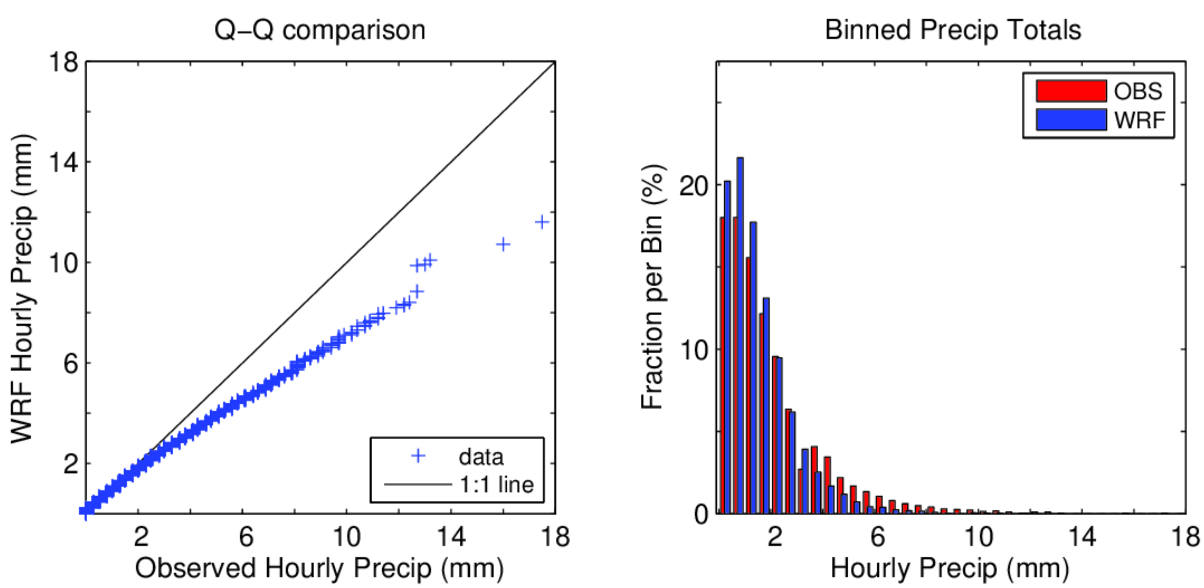

Figure 5. Quantile-Quantile (“Q-Q” comparison, left) and binned precipitation totals (right, 0-0.5 mm/hr, 0.5-1.0 mm/hr, etc.) for Sea-Tac and the nearest WRF-NARR grid cell.

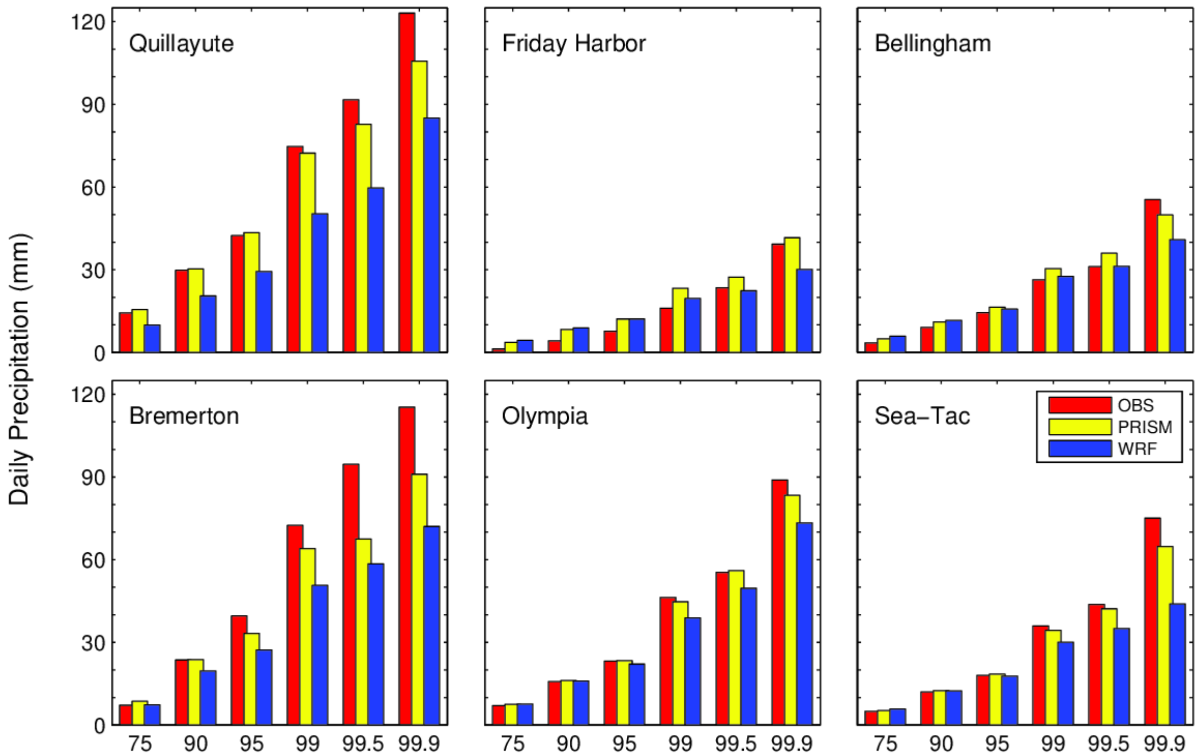

Figure 6. Comparing select quantiles in daily precipitation for the ASOS stations, PRISM, and WRF-NARR. Results are shown for the six ASOS stations shown in Figure 1.

all locations. Unlike the comparisons in Figures 4 and 5, these are based on daily precipitation, since the PRISM data is provided at a daily time step. Notably, the PRISM and ASOS results are not exactly in agreement. This could be due to the grid cell locations for PRISM, which do not align exactly with the ASOS locations, but could also reflect inaccuracies in the PRISM model. As noted above, another potential source of disagreement is the different resolution of the PRISM and WRF-NARR models. Regardless, since the PRISM model is our best option for gridded corrections, these disagreements with ASOS should be taken into consideration when using our results.

Bias Correction

We used daily PRISM data to bias-correct the WRF-NARR simulations. Although PRISM does not always agree with the ASOS observations, it is currently our best option for applying a spatially distributed correction. We opted to apply the "percentile-delta" bias correction described above, since the results above suggest that biases are not the same across all quantiles. Corrections were calculated as multiplicative scalars (e.g. multiplying by 1.11 to correct for a 10% dry bias). Since PRISM data is daily, we calculated a correction for each day, then applied it uniformly to all hours within that day. To avoid over-correcting, we did not allow corrections larger than +100% (a factor of 2); we find that this is only the case for the low intensity bins.

Since stormwater design is particularly sensitive to moderate and high intensity precipitation events, we tested three versions of the "percentile-delta" approach in which

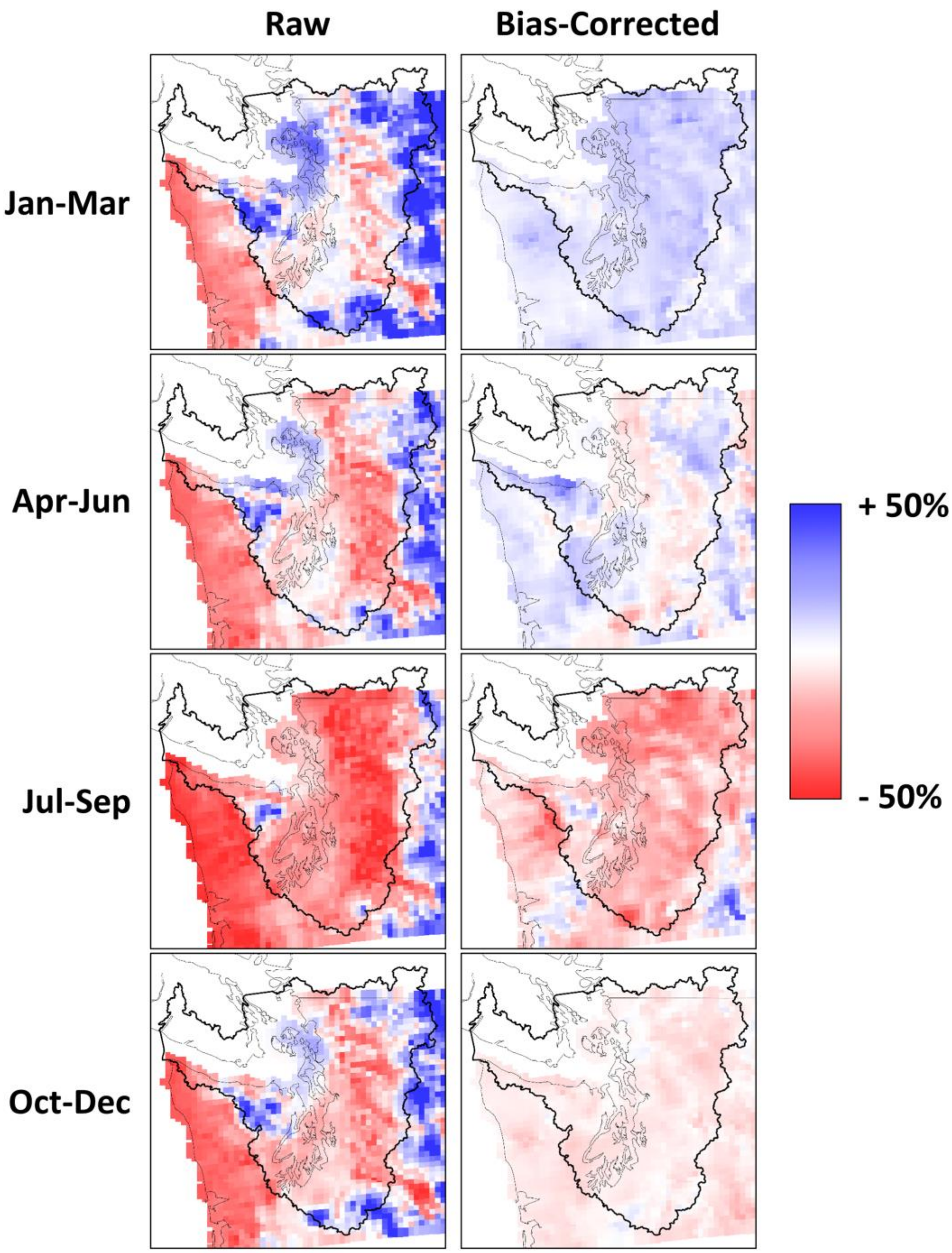

Figure 7. Percent bias in seasonal total precipitation for WRF-NARR relative to PRISM.

the bin size was varied from 0.25 to 0.5 to 1.0 percentile per bin. Although not shown here, we found no appreciable difference between the three approaches. As a result we selected the largest bin size (1.0 percentile) in order to maximize the sample size within each bin. All of the comparisons in this section show results for this bin size.

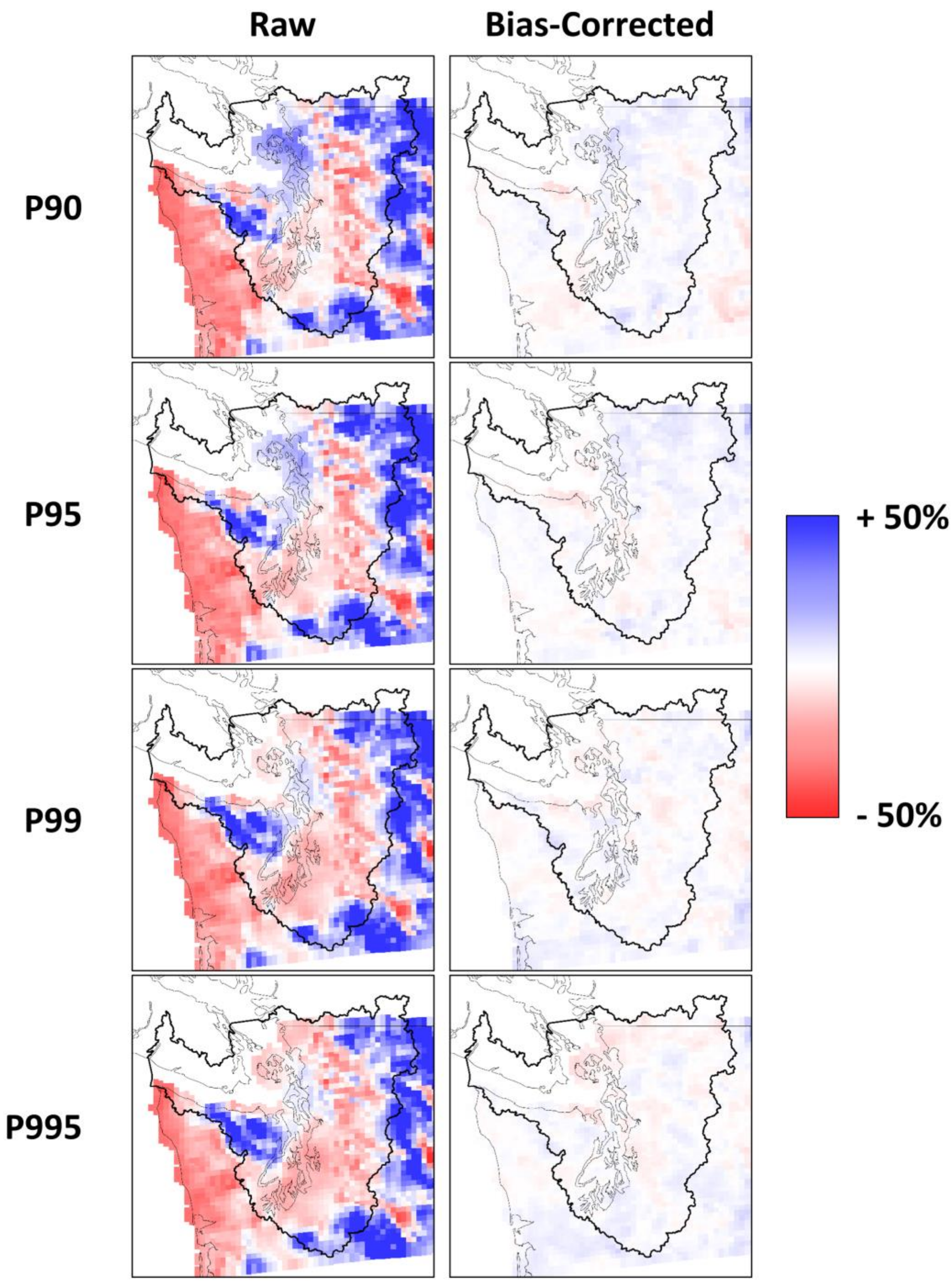

Figure 8. As in Figure 7 except showing biases in the 90th, 95th, 99th, and 99.5th percentiles in daily precipitation.

Figures 7 and 8 compare the WRF-NARR biases for seasonal precipitation and the same four quantiles in daily precipitation, respectively. These show dramatic improvements between the uncorrected ("raw") and bias-corrected WRF-NARR results. Although biases are not eliminated with our approach, they are reduced to within approximately 10% of the PRISM estimates for all of the precipitation quantiles. Biases for seasonal precipitation are also reduced, but not as dramatically as for the daily quantiles. Larger biases are expected for the seasonal totals since the bias-correction is applied to daily precipitation and does not directly address seasonal totals. Nonetheless, the biases in the seasonal totals are significantly improved with the correction.

In order to better inspect the corrections, we show the point comparisons for the same locations evaluated in the previous section. Figure 9 shows Q-Q plots comparing daily PRISM precipitation (x-axes) to both the uncorrected (raw) and bias-corrected (bc) WRF-NARR results. In order to better view biases across all quantiles, the plots compare the log-transformed precipitation. These confirm that the bias-correction successfully corrects the biases across all but the lowest and highest quantiles. For the extreme values, the binning

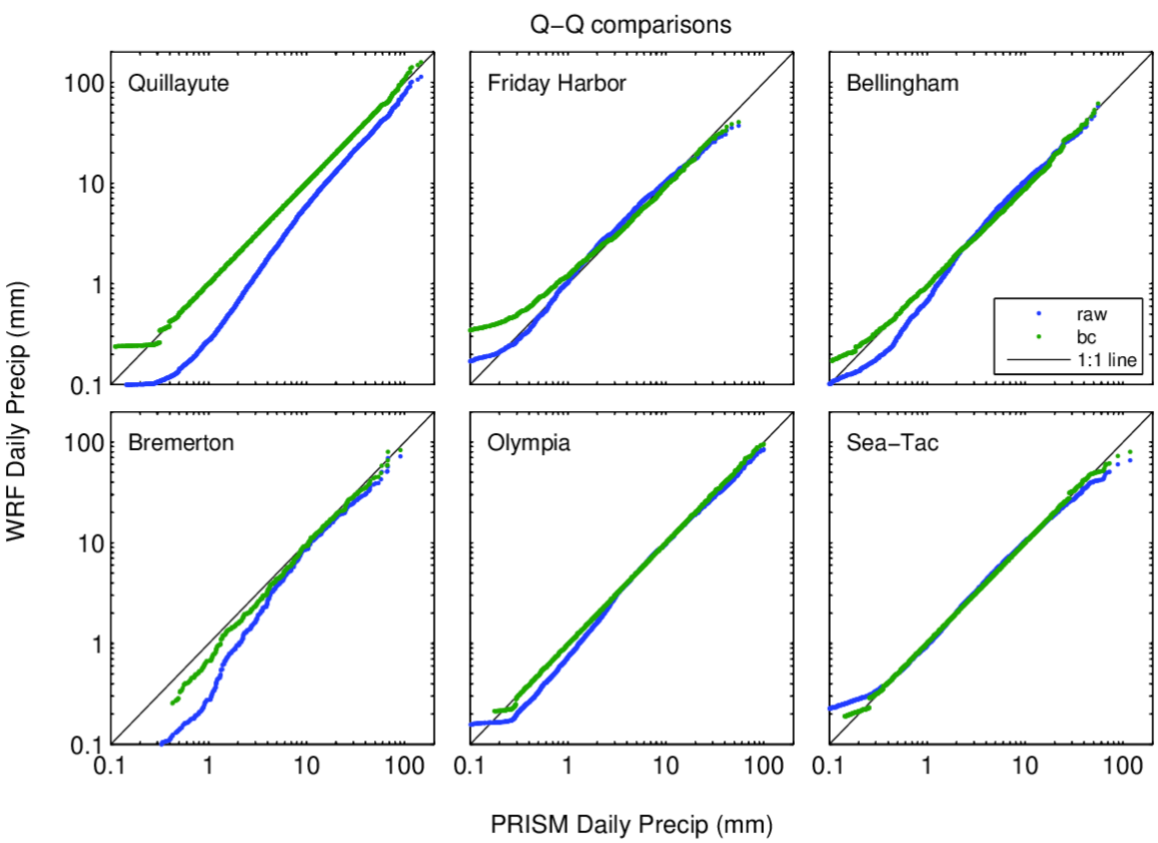

Figure 9. Quantile-Quantile (Q-Q) comparisons of daily precipitation (mm) between PRISM (x-axes) and both uncorrected ("raw") and bias-corrected ("bc") WRF-NARR, for the six ASOS stations shown in Figure 1.

used in our percentile-delta approach does not fully resolve the differences in bias. An additional reason for persistent biases is that we capped the scalings at a factor of two. This likely explains the remaining biases across lower quantiles at the Bremerton location, for which the uncorrected WRF-NARR results are biased low by more than a factor of two. Finally, we note that since the PRISM precipitation estimates differ from the ASOS observations, our corrections do not necessarily lead to reductions in the biases relative to ASOS. In addition, the corrections are applied to daily precipitation as opposed to hourly precipitation, which may mean that biases in the hourly estimates remain.

References

Brekke, L. D., Dettinger, M. D., Maurer, E. P., & Anderson, M. (2008). Significance of model credibility in estimating climate projection distributions for regional hydroclimatological risk assessments. Climatic Change, 89(3), 371-394. https://doi.org/10.1007/s10584-007-9388-3

Brewer, M. C., & Mass, C. F. (2016). Projected changes in western US large-scale summer synoptic circulations and variability in CMIP5 models. Journal of Climate, 29(16), 5965-5978. https://doi.org/10.1175/JCLI-D-15-0598.1

Chen, X., Leung, L. R., Gao, Y., Liu, Y., Wigmosta, M., & Richmond, M. (2018). Predictability of extreme precipitation in western US watersheds based on atmospheric river occurrence, intensity, and duration. Geophysical Research Letters, 45(21), 11-693.

Daly, C., M. Halbleib, J.I. Smith, W.P. Gibson, M.K. Doggett, G.H. Taylor, J. Curtis, and P.A. Pasteris. 2008. Physiographically-sensitive mapping of temperature and precipitation across the conterminous United States. International Journal of Climatology 28(15): 2031-2064. doi:10.1002/joc.1688

Daly, C., Doggett, M. K., Smith, J. I., Olson, K. V., Halbleib, M. D., Dimcovic, Z., ... & Kaspar, E. M. (2021). Challenges in observation-based mapping of daily precipitation across the conterminous United States. Journal of Atmospheric and Oceanic Technology, 38(11), 1979-1992.

Department of Ecology. 2014. “Stormwater Management Manual for Western Washington,” 1192.

Dinicola, Richard S. 1990. “Characterization and simulation of rainfall-runoff relations for headwater basins in western King and Snohomish Counties, Washington.” Water-Resources Investigations Report 89-4052: 52 p. https://pubs.er.usgs.gov/publication/wri894052

Dulière, V., Zhang, Y., & Salathé Jr, E. P. (2011). Extreme precipitation and temperature over the US Pacific Northwest: A comparison between observations, reanalysis data, and regional models. Journal of Climate, 24(7), 1950-1964.

Huffman, G.J., Bolvin D.T., Braithwaite, D., Hsu, K., Joyce, R., Kidd, C., Nelkin, E.J., Sorooshian, S., Tan, J., Xie, P. (2018). Algorithm Theoretical Basis Document (ATBD) Version 5.2: NASA Global Precipitation Measurement (GPM) Integrated Multi-satellitE Retrievals for GPM (IMERG). Prepared for: Global Precipitation Measurement (GPM), National Aeronautics and Space Administration (NASA). https://docserver.gesdisc.eosdis.nasa.gov/public/project/GPM/IMERG_ATBD_V06.pdf

Kao, S. C., DeNeale, S. T., Yegorova, E., Kanney, J., & Carr, M. L. (2020). Variability of precipitation areal reduction factors in the conterminous United States. Journal of Hydrology X, 9, 100064. https://doi.org/10.1016/j.hydroa.2020.100064

Liu, C., Ikeda, K., Rasmussen, R., Barlage, M., Newman, A. J., Prein, A. F., ... & Yates, D. (2017). Continental-scale convection-permitting modeling of the current and future climate of North America. Climate Dynamics, 49, 71-95. https://doi.org/10.1007/s00382-016-3327-9

Lorente-Plazas, R., Mitchell, T. P., Mauger, G., & Salathé, E. P. (2018). Local enhancement of extreme precipitation during atmospheric rivers as simulated in a regional climate model. Journal of Hydrometeorology, 19(9), 1429-1446.

Mauger, G.S., S.-Y. Lee, C. Bandaragoda, Y. Serra, J.S. Won, 2016. Refined Estimates of Climate Change Affected Hydrology in the Chehalis basin. Report prepared for Anchor QEA, LLC. Climate Impacts Group, University of Washington, Seattle. https://doi.org/10.7915/CIG53F4MH

Mauger, G.S., J.S. Won, K. Hegewisch, C. Lynch, R. Lorente Plazas, E. P. Salathé Jr., 2018. New Projections of Changing Heavy Precipitation in King County. Report prepared for the King County Department of Natural Resources. Climate Impacts Group, University of Washington, Seattle.

Mauger, G.S., J.S. Won, 2019. Expanding the ensemble of precipitation projections for King County. Report prepared for the King County Department of Natural Resources. Climate Impacts Group, University of Washington, Seattle.

Mauger, G.S., J. Robinson, R.J. Mitchell, J. Won, and N. Cristea (2021). Climate Change & Flooding in Snohomish County: New Dynamically-Downscaled Hydrologic Model Projections. Report prepared for Snohomish County. Climate Impacts Group, University of Washington. https://doi.org/10.6069/SQJ2-DF62

Mass, C. F., Salathé Jr, E. P., Steed, R., & Baars, J. (2022). The mesoscale response to global warming over the Pacific Northwest evaluated using a regional climate model ensemble. Journal of Climate, 35(6), 2035-2053.

Nelson, B. R., Prat, O. P., Seo, D. J., & Habib, E. (2016). Assessment and implications of NCEP Stage IV quantitative precipitation estimates for product intercomparisons. Weather and Forecasting, 31(2), 371-394. https://doi.org/10.1175/WAF-D-14-00112.1

Ransom, J. I., M. Krosby, and A. L. Lyons. 2018. Climate change implications for grizzly bears (Ursus arctos) in the North Cascades Ecosystem. Natural Resource Report NPS/NOCA/NRR— 2018/1814. National Park Service, Fort Collins, Colorado.

Rasmussen, R. M., Chen, F., Liu, C. H., Ikeda, K., Prein, A., Kim, J., ... & Miguez-Macho, G. (2023). CONUS404: The NCAR–USGS 4-km long-term regional hydroclimate reanalysis over the CONUS. Bulletin of the American Meteorological Society, 104(8), E1382-E1408. https://doi.org/10.1175/BAMS-D-21-0326.1

Rupp, D. E., Abatzoglou, J. T., Hegewisch, K. C., & Mote, P. W. (2013). Evaluation of CMIP5 20th century climate simulations for the Pacific Northwest USA. Journal of Geophysical Research: Atmospheres, 118(19), 10-884. https://doi.org/10.1002/jgrd.50843

Salathé, E. P., Leung, L. R., Qian, Y., & Zhang, Y. (2010). Regional climate model projections for the State of Washington. Climatic Change, 102, 51-75.

Salathé Jr, E. P., Hamlet, A. F., Mass, C. F., Lee, S. Y., Stumbaugh, M., & Steed, R. (2014). Estimates of twenty-first-century flood risk in the Pacific Northwest based on regional climate model simulations. Journal of Hydrometeorology, 15(5), 1881-1899.

Skamarock, W. C., Klemp, J. B., Dudhia, J., Gill, D. O., Barker, D. M., Duda, M. G., ... & Powers, J. G. (2008). A description of the advanced research WRF version 3, NCAR Technical Note. National Center for Atmospheric Research: Boulder, CO, USA.

Taylor, K. E., Stouffer, R. J., & Meehl, G. A. (2012). An overview of CMIP5 and the experiment design. Bulletin of the American meteorological Society, 93(4), 485-498.

Van Vuuren, D. P., Edmonds, J., Kainuma, M., Riahi, K., Thomson, A., Hibbard, K., ... & Rose, S. K. (2011). The representative concentration pathways: an overview. Climatic change, 109(1), 5-31.